Title
GADD34 Function in Protein Trafficking Promotes Adaptation to Hyperosmotic Stress in Human Corneal Cells

Journal
Cell Reports, 21(10)

ISSN
2639-1856

Authors
Krokowski, Dawid
Guan, Bo-Jhih
Wu, Jing
et al.

Publication Date
2017-12-01

DOI
10.1016/j.celrep.2017.11.027

Peer reviewed

HHS Public Access

Author manuscript

Cell Rep. Author manuscript; available in PMC 2017 December 07.

Published in final edited form as:

Cell Rep. 2017 December 05; 21(10): 2895–2910. doi:10.1016/j.celrep.2017.11.027.

GADD34 function in protein trafficking promotes adaptation to hyperosmotic stress in human corneal cells

Dawid Krokowski[1,#], **Bo-Jhih Guan**[1], **Jing Wu**[1], **Yuke Zheng**[1], **Padmanabhan P. Pattabiraman**[2], **Raul Jobava**[1], **Xing-Huang Gao**[1], **Xiao-Jing Di**[3], **Martin D. Snider**[4], **Ting-Wei Mu**[3], **Shijie Liu**[5], **Brian Storrie**[5], **Eric Pearlman**[6], **Anna Blumental-Perry**[7,#], and **Maria Hatzoglou**[1,#,$]

[1]Department of Genetics and Genome Sciences, Western Reserve University, Cleveland, OH, 44106, USA

[2]Department of Ophthalmology and Visual Science Case, Western Reserve University, Cleveland, OH, 44106, USA

[3]Department of Physiology and Biophysics, Western Reserve University, Cleveland, OH, 44106, USA

[4]Department of Biochemistry, Western Reserve University, Cleveland, OH, 44106, USA

[5]Department of Physiology and Biophysics, University of Arkansas for Medical Sciences, Little Rock, AR, 72205, USA

[6]Institute for Immunology, University of California, Irvine, CA, 92697, USA

[7]Department of Surgery, Western Reserve University, Cleveland, OH, 44106, USA

Summary

GADD34, a stress-induced regulatory subunit of the phosphatase PP1, is known to function in hyperosmotic stress through its well-known role in the Integrated Stress Response pathway (ISR). Adaptation to hyperosmotic stress is important for the health of corneal epithelial cells exposed to changes in extracellular osmolarity, with maladaptation leading to dry eye syndrome. This adaptation includes induction of SNAT2, an ER-Golgi processed protein, which helps to reverse stress-induced loss of cell volume and promote homeostasis through amino acid uptake. Here, we show that GADD34 promotes processing of proteins synthesized on the endoplasmic reticulum during hyperosmotic stress independent of its action in the ISR. We show that GADD34/PP1

[#]To whom correspondence should be addressed: Maria Hatzoglou, Department of Genetics and Genome Sciences, Case Western Reserve University, 10900 Euclid Avenue, Cleveland, OH 44106, USA; Tel: 216-368- 3012; Fax: 216-368-4095; mxh8@case.edu. Dawid Krokowski, Department of Genetics and Genome Sciences, Case Western Reserve University; dmk102@case.edu. Anna Blumental-Perry, Department of Surgery, Case Western Reserve University; axb811@case.edu.
[$]Lead contact

Author Contributions

D.K. and M.H. designed the study. A.B.P advised on trafficking experiments. D.K., B.J.G., J.W., Y.Z., K.F., R.J. P.P.P., S.L., X.G., and A.B.P. performed experiments. A.B.P., P.P.P., T.M., X.D., and B.S. provided expertise with fluorescence microscopy. E.P. provided important reagents. D.K., A.B.P., M.D.S. and M.H. wrote the article.

phosphatase activity reverses hyperosmotic stress-induced Golgi fragmentation and is important for cis- to trans-Golgi trafficking of SNAT2, thereby promoting SNAT2 plasma membrane localization and function. These results suggest that GADD34 is a protective molecule for ocular diseases such as dry eye syndrome.

eTOC Blurb

Here, Krokowski et al. show that GADD34/PP1 protects the microtubule network, prevents Golgi fragmentation, and preserves protein trafficking independent of its action in the Integrated Stress Response (ISR). In osmoadaptation, GADD34 facilitates *trans*-Golgi-mediated processing of the ER-synthesized amino acid transporter SNAT2, which in turn increases amino acid uptake.

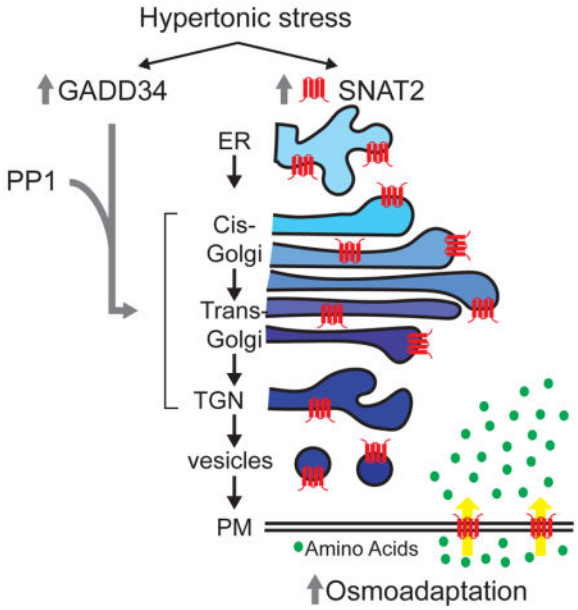

Introduction

Homeostasis in tissues exposed to significant changes in osmolarity (Brocker et al., 2012) is maintained through an adaptive cellular response. Failure of adaptation is implicated in the development of various pathophysiological conditions. Among the most prominent is dry eye syndrome (Bhavsar et al., 2011), where hyperosmolarity of the tear film, can be linked to both inflammation and corneal cell loss due to apoptosis (Lam et al., 2009; Lin et al., 2011; Luo et al., 2007; Yeh et al., 2003). Understanding the mechanisms of adaptation to hyperosmotic stress is a key to the development of therapeutic approaches to treat dry eye syndrome and related diseases (Brocker et al., 2012). Initial stress-induced cell shrinkage activates Na^+/H^+ exchangers of the Slc9 transporters family, Na^+, K^+, $2Cl^-$ cotransporters of the Slc12 family (Eveloff and Warnock, 1987; Pedersen et al., 2007), and possibly increased uptake of extracellular Ca^{2+}, all of which contribute to regulatory volume increase (RVI) (Burg et al., 2007; Lang et al., 1998; Sanchez and Wilkins, 2004). This initial RVI response does not require *de novo* protein synthesis. A second phase replaces these inorganic ions by increasing the pool of intracellular organic osmolytes (Burg et al., 2007; Franchi-Gazzola et

al., 2006). This second phase requires synthesis of proteins mediating the uptake and biosynthesis of osmolytes (Dall'Asta et al., 1994; Franchi-Gazzola et al., 2006). Among these is the amino acid transporter, SNAT2, which mediates the concentrative uptake of small neutral amino acids, which act as osmolytes to maintain RVI (Broer, 2014).

Osmoadaptation has been studied extensively at the level of transcriptional control (Burg et al., 2007), and to a lesser extent at the level of regulation of protein synthesis. A signaling pathway, which regulates protein synthesis in diverse stress conditions is the phosphorylation of the translation initiation factor eIF2α, known as the Integrated Stress Response (ISR). Phosphorylation of eIF2α causes a decrease in global protein synthesis, and at the same time induces translational reprogramming that leads to adaptation to stress conditions. An important component of this response is the induction of GADD34, a regulatory subunit of the protein phosphatase PP1 that dephosphorylates eIF2α-P (Novoa et al., 2001). This dephosphorylation restores protein synthesis and allows execution of the stress-induced transcription programs. The cellular response to hyperosmotic stress also involves eIF2α-P/GADD34 signaling (Bevilacqua et al., 2010; Krokowski et al., 2015). However, inhibition of protein synthesis during hyperosmotic stress involves mechanisms beyond the regulation of the phosphorylation status of eIF2α (Czech et al., 2013). Our previous studies showed that GADD34 and SNAT2 during hyperosmotic stress are co-regulated (Bevilacqua et al., 2010; Krokowski et al., 2015). These studies in MEFs suggested a molecular interplay between the eIF2α-P/GADD34 axis and the SNAT2 protein (Krokowski et al., 2015).

The current study has used a human corneal epithelial cells, and MEFs deficient in eIF2α phosphorylation (S51A) to reveal a function of GADD34/PP1 in osmoadaptation. Increased osmolarity caused transient fragmentation of the Golgi apparatus and GADD34/PP1 reversed this fragmentation. Mild stress in parallel to Golgi fragmentation induced changes in the microtubular network with transient dissociation of microtubules from the cortical actin network. Adaptation to stress reversed these changes in microtubules. This rebuilding of the microtubule network was sensitive to GADD34/PP1 inhibition. Moreover, GADD34/PP1 was also shown to be important for Golgi integrity in basal conditions in the absence of stress. The osmoprotective induction and localization of SNAT2 to the plasma membrane (PM) was attenuated in cells with inactive GADD34/PP1. Inhibition of GADD34/PP1 activity during stress resulted in SNAT2 accumulation in the *cis*-Golgi compartment, thus affecting the terminal steps of maturation and functional SNAT2 membrane localization. We conclude that the molecular interplay between GADD34/PP1 and SNAT2 is an important post-translational mechanism of the adaptive response to hyperosmotic stress. Functions of GADD34/PP1 in SNAT2 trafficking, Golgi integrity, and microtubule network maintenance are described here for the first time, and are independent of the role of GADD34/PP1 in the well-studied ISR (Novoa et al., 2001). A more global view of the GADD34-mediated effects on the trafficking of proteins from the ER to PM was obtained with the retention using selective hooks (RUSH) experimental system (Boncompain et al., 2012). We have used the RUSH methodology to demonstrate a slower delivery of a reporter protein from the ER to PM in GADD34$^{\Delta C/\Delta C}$ MEFs. The combined data conclude that the activity of GADD34/PP1 assists trafficking/maturation of proteins from the ER to Golgi to the PM. GADD34/PP1 inhibitors are currently being developed as

therapeutics for neurodegenerative and other diseases (Das et al., 2015), the discovery of these functions of GADD34/PP1 introduces additional important considerations in the design of clinical protocols.

Results

Adaptation to increased extracellular osmolality depends on stress intensity

The corneal epithelium is composed of highly specialized cells. We used cultured human corneal epithelial cells to study the response to increased osmolarity of media containing NaCl. This experimental system mimics the hyperosmotic tear film that causes dry eye syndrome (Bhavsar et al., 2011; Stahl et al., 2012). We tested the levels of SNAT2 in cells exposed to mild (500 mOsm) or severe (600 mOsm) stress. These two stress conditions were chosen based on our previous reports that cells adapt to mild stress but not to severe stress (Bevilacqua et al., 2010; Krokowski et al., 2015). SNAT2 mRNA levels were gradually induced by mild stress similar to MEFs (Krokowski et al., 2015) but induction was absent in severe stress (Fig. 1A). Increased SNAT2 mRNA was reflected in higher uptake of its substrate methylaminoisobutyric acid (MeAIB; Fig. 1B) and accumulation of transporter protein (Fig. 1C) during mild but not severe stress. We have shown previously that SNAT2 expression in MEFs is coordinated with induction of GADD34 (Krokowski et al., 2015); a similar regulation was observed in corneal epithelial cells exposed to 500 mOsm, but not 600 mOsm media (Fig. 1A,C).

Induction of SNAT2 is an important element of the adaptation program in corneal epithelial cells

We first examined the role of SNAT2 in preventing hyperosmotic stress-induced apoptosis. Severe hyperosmotic stress in MEFs decreases cell viability through induction of apoptosis via the intrinsic pathway (Bevilacqua et al., 2010; Saikia et al., 2014). Similarly, in corneal epithelial cells, apoptosis was induced by severe, but not mild stress, as demonstrated by increases in the proteolytic cleavage of PARP and caspase 3 and the activity of caspase 3 (Fig. S1A,B). We tested the importance of SNAT2 in protecting cells from apoptosis during mild stress by depleting SNAT2 mRNA through the use of SNAT2-directed shRNA. SNAT2 depletion inhibited the induction of both SNAT2-mediated transport and SNAT2 protein levels during mild stress (Fig. S1C,D). This reduction in stress-induced SNAT2 expression resulted in an increase in caspase 3 cleavage and activity (Fig. S1D,E). We also found that absence of SNAT2 expression induces more caspase 3 cleavage and higher caspase 3 activity at earlier time points during the treatment of corneal epithelial cells with severe stress (Fig. S1F,G). Under severe stress conditions, although SNAT2 mRNA is not induced (Fig. 1A), its sustained basal levels offer protection from the early induction of apoptosis. Our data support the importance of SNAT2 in corneal epithelial cell osmoadaptation.

Maturation of the SNAT2 protein requires active GADD34/PP1

The uptake of neutral amino acids by SNAT2 is crucial for adaptation to hyperosmolar conditions in corneal epithelial cells (Fig. S1) and in MEFs (Bevilacqua et al., 2005; Franchi-Gazzola et al., 2006). We showed previously that GADD34 expression had no impact on the levels of SNAT2 mRNA or its association with translating ribosomes,

suggesting that translation of this mRNA is insensitive to the stress-induced inhibition of protein synthesis (Krokowski et al., 2015). Conceivably, the well-characterized ability of GADD34/PP1 to dephosphorylate eIF2α-P and reactivate translation during different stress conditions (Novoa et al., 2001) may not be important for SNAT2 expression. To test this directly, we used GADD34/PP1 inhibitors. Sal003, a salubrinal (Sal) derivative that inhibits the phosphatase activity of GADD34/PP1 (Boyce et al., 2005), caused an increase in eIF2α-P (Fig. S2A). Sal003 also inhibited the increase in SNAT2 transport activity caused by hyperosmotic stress in a dose-dependent manner (Fig. S2B). Sal003 inhibits dephosphorylation of eIF2α-P by targeting the interaction of PP1 with either CReP or GADD34 regulatory subunits (Hetz et al., 2013). To determine which subunit is important for SNAT2 expression, we tested the effects of Guanabenz (Guan) and Sephin 1 (Seph), which target GADD34/PP1 but not CReP/PP1 (Carrara et al., 2017; Das et al., 2015; Hetz et al., 2015; Tsaytler et al., 2011). These inhibitors have similar structures; however, Guanabenz is also a potent agonist of the α2-adrenergic receptor (Das et al., 2015; Tsaytler et al., 2011). Because this receptor has been reported in corneal epithelial cells (Grueb et al., 2008), we studied both compounds to exclude any contribution of adrenergic signaling. GADD34/PP1 inhibitors showed dose-dependent inhibition of the hyperosmolarity-induced SNAT2 transport activity (Fig. S2C). None of these inhibitors significantly affected SNAT2 mRNA induction (Fig. S2D).

We next tested if SNAT2 plasma membrane localization in corneal epithelial cells, requires GADD34/PP1 activity. Sal003 treatment decreased the accumulation of mature SNAT2 protein at the PM in corneal epithelial cells, as evident from analysis of total membrane fractions (Fig. 1D) and fractions of proteins biotinylated on the cell surface (Fig. 1E,F). In agreement with our biochemical data, hyperosmotic stress led to an increase in SNAT2 signal with a significant fraction visible on the cell surface (Fig. 1G, S2E). Inhibition of the GADD34/PP1 function by Sal003 treatment resulted in a dramatic decrease in SNAT2 delivery to cell surface (Fig. 1G, S2E), a decrease in SNAT2-mediated amino acid uptake (Fig. S2B), and levels of mature SNAT2 protein (Fig 1D–E).

To confirm that the effects of Sal003 are specific to GADD34/PP1, we depleted the GADD34 protein using shRNA. Introduction of GADD34 shRNA into cells resulted in a decrease in stress-induced expression of GADD34 mRNA and protein (Fig. S3A,C), but had no effect on the levels of SNAT2 mRNA, indicating that GADD34 is not involved in the regulation of SNAT2 gene expression (Fig. S3A). Even though GADD34 shRNA did not affect SNAT2 mRNA levels, there was inhibition of the stress-induced increase in transport activity (Fig. S3B). A decrease in protein levels was observed when Western blots of whole cell lysates and membrane fractions were analyzed (Fig. S3C–E). Finally, downregulation of GADD34 expression led to an increase in apoptosis, as evidenced by increased caspase 3 cleavage and caspase 3 activity (Fig. S3C,F). These data emphasize the adaptive functions of GADD34 during hyperosmotic stress.

To delineate the precise mechanism of action of GADD34 on SNAT2 protein maturation in corneal epithelial cells, we analyzed the presence of different forms of SNAT2 resolved in SDS/PAGE gels from cells in which GADD34/PP1 activity was inhibited. Addition of Sal003 resulted in a decrease in mature SNAT2 protein and an increase in a faster-migrating

species (Fig. 2A). The two forms of SNAT2 differ in their N-linked glycosylation status: the faster-migrating form corresponds to the ER-processed SNAT2 with endo-H sensitive glycans (Freeze and Kranz, 2010)(immature SNAT2), while the slower-migrating form corresponds to the Golgi-localized SNAT2 with further processed endo-H resistant glycans (Freeze and Kranz, 2010)(mature SNAT2)(Fig. 2A). To confirm the identity of the rapidly-migrating form, we used inhibitors of protein glycosylation and intracellular trafficking. Addition of Tunicamycin (Tu), which blocks the assembly of N-linked glycans in the ER, caused accumulation of the fastest migrating form of SNAT2, consistent with the inhibition of N-linked glycosylation (Fig. 2A marked as unglycosylated). Addition of inhibitors of COPI vesicle formation (Brefeldin A [BFA] and Golgicide A [GCA]), caused the pronounced accumulation of ER-glycosylated SNAT2 species relative to the that observed with Sal003 treatment (Fig. 2A). In brief, all of these inhibitors had an effect on intracellular SNAT2 trafficking to the *trans*-Golgi-located glycosyltransferases, which would modify the protein to form mature SNAT2 (Fig. 2A).

Next we examined how inhibition of GADD34/PP1 affects the SNAT2 distribution within the secretory pathway. Addition of Sal003 during hyperosmotic treatment increased the levels of immature protein (Fig. 2A–C) suggesting a retention of SNAT2 in compartments proximal to *trans*-Golgi, where terminal glycosylation occurs. Retention of the protein in the ER would make it a substrate for Endoplasmic-Reticulum-Associated protein Degradation (ERAD; (Ruggiano et al., 2014). To evaluate the potential contribution of ERAD to clearance of SNAT2 from the ER compartment, we used the proteasome inhibitor MG132, which blocks the final degradation steps. MG132 caused an accumulation of unglycosylated SNAT2 and the expected increase in levels of ubiquitinated proteins. The accumulation of unglycosylated SNAT2 was only observed in MG132-treated cells, suggesting that any unglycosylated intermediate is normally cleared rapidly by the proteasome. Nevertheless, MG132 did not affect the level of immature ER-glycosylated SNAT2 in stressed cells with or without GADD34/PP1 inhibition (Fig. 2B,C), suggesting that this form is not degraded by ERAD.

These data are consistent with the idea that Sal003 treatment does not induce accumulation of the immature form in the ER compartment. To further confirm this notion, we examined the effects of hyperosmotic stress and Sal003 on SNAT2 distribution using immunofluorescence microscopy. Cells were stained for SNAT2 (green) and the ER-marker KDEL (red). KDEL staining showed the characteristic pattern for ER—reticular staining with perinuclear concentration. None of the treatments used significantly affected KDEL distribution. SNAT2 staining was weak in untreated cells and in control cells treated with Sal003 (Fig. 2D). It consisted of punctate structures with little to no co-localization to KDEL staining (Fig. 2D,E). Hyperosmotic stress resulted in significant increase in SNAT2 staining intensity and redistribution of SNAT2 to vesicular structures, which do not co-localize with KDEL and possibly correspond to SNAT2 post-Golgi trafficking and PM localization (Fig. 2E, white arrowheads). Addition of Sal003 to cells experiencing hyperosmotic stress neither affected the increase in SNAT2 intensity nor induced its significant retention in the ER, but it did block SNAT2 trafficking to the PM (Fig. 2D–F). Therefore, ER-retention of SNAT2 in cells lacking functional GADD34/PP1 cannot account for the accumulation of immature transporter during hyperosmotic stress. The majority of

SNAT2 in stress conditions with or without Sal003 is localized outside of the ER in Golgi-like structures.

GADD34/PP1 is involved in maintaining Golgi integrity

To further understand the mechanism of action of GADD34/PP1 on SNAT2 post-ER processing during hyperosmotic stress, we examined Golgi morphology and SNAT2 distribution in cells with or without active GADD34/PP1. Our analysis of SNAT2 protein during adaptation to hyperosmotic stress emphasized the importance of its intracellular transport and glycosylation. Because the Golgi complex is vital for trafficking of SNAT2 to the PM, we examined the effect of hyperosmotic stress on Golgi morphology using GM130 as a Golgi marker. Hyperosmotic stress induced Golgi fragmentation (Fig. 3A), and the percentage of cells with fragmented Golgi complexes increased with stress intensity (Fig. 3B). The fragmentation during mild stress was transient; after the initial increase in fragmentation at 1h, the Golgi complex partially recovered its morphology (Fig. 3C). This recovery corresponded with the timing of SNAT2 and GADD34 induction (Fig. 3C, 1A–C). Therefore, we conclude that during mild stress, the initial fragmentation of Golgi is followed by a recovery that correlates with the expression of the osmoprotective membrane protein SNAT2.

Because GADD34/PP1 is required for the stress-induced expression and maturation of SNAT2 (Fig. 1D–G, S2, S3), we studied its effects on Golgi fragmentation. Silencing of GADD34 expression by shRNA increased the number of cells with fragmented Golgi in both control and hyperosmotic media (Fig. 3D, S3G). The effect of GADD34 silencing was most evident after prolonged stress, when physiological GADD34 levels are induced to support the adaptation to stress. In agreement with a role of GADD34/PP1 in maintaining Golgi morphology, the addition of GADD34/PP1 inhibitors Sal003 and Sephin 1 caused a dose-dependent increase in Golgi fragmentation in control cells (Fig. 3E), with Sal003 having a more prominent effect. Sephin 1 is a very selective GADD34/PP1 inhibitor (Carrara et al., 2017; Das et al., 2015); in contrast, Sal003 has an additional inhibitory effect on PP1 when, instead of GADD34, it contains the constitutively-expressed regulatory subunit CReP (Choy et al., 2015). We next tested if the effects of GADD34/PP1 on Golgi fragmentation involve the well-known eIF2α-P-mediated responses in ISR. It is well established that GADD34 during the ISR, promotes dephosphorylation of eIF2α-P with the subsequent reversal of the eIF2α-P-mediated stress-induced reprogramming of the cells, including the reversal of induction of the master regulator of the stress response, the transcription factor ATF4 (Novoa et al., 2001; Sidrauski et al., 2015). The integrated stress response inhibitor (ISRIB) has been shown to reverse the eIF2α-P-mediated stress-induced effects, independently of the actions of GADD34/PP1 (Di Prisco et al., 2014; Sidrauski et al., 2015). If the GADD34/PP1 effects on Golgi fragmentation during hyperosmotic stress are independent of its target eIF2α-P, treatment of cells with ISRIB should not reverse Sephin 1-induced Golgi fragmentation. Treatment of cells with ISRIB combined with Sephin 1, did not prevent the induction of fragmented Golgi (Fig. 3F). As expected (Sidrauski et al., 2015), ISRIB treatment of corneal cells during Thapsigargin (Tg)-induced ER stress, reversed induction of ATF4, but not the non ISR-mediated splicing of XBP1

mRNA (Fig. S3H). Taken together, inhibition of GADD34/PP1 induces Golgi fragmentation via mechanisms that do not involve the eIF2α-P-mediated effects in ISR.

Both microtubules and actin filaments undergo dynamic changes in response to cell shrinkage induced by hyperosmolarity (Nunes et al., 2013; Yamamoto et al., 2006). Fitness of the Golgi apparatus, including proper cellular distribution of Golgi cisterns and transport events which couple microtubules and motor proteins that drive motility, rely on the proper assembly of microtubules (Allan et al., 2002). We therefore investigated changes in the microtubule and actin networks in corneal cells exposed to hyperosmotic stress. In untreated cells, actin exhibited peripheral accumulation in cortical rims and actin stress fibers (Fig. 3G). The microtubules were distributed across the cytoplasm and extended to the PM (Fig. 3H). Shortly after exposure to hyperosmotic stress we observed an increase in actin stress fibers and a decrease in microfilaments interacting with the PM. These cytoskeletal network changes were reversed during longer stress treatment (Fig. 3G) and this reversal was inhibited by the treatment of cells during stress with the GADD34/PP1 inhibitor, Sephin 1 (Fig. 3G,H). These data suggest an involvement of GADD34 in the regulation of tubulin polymerization, which can also explain its functions on maintaining Golgi integrity.

Our results point to the importance of GADD34/PP1 in promoting Golgi integrity under both basal conditions and during adaptation to stress. It is possible that the action of GADD34/PP1 via unknown targets is necessary to reverse the initially high Golgi fragmentation as part of the mechanism that promotes SNAT2 maturation and PM-localized activity.

Induction of Golgi fragmentation results in decreased SNAT2 expression and processing during hyperosmotic stress

The regulated fragmentation of the Golgi during mild hyperosmotic stress reveals a mechanism of osmoadaptation via the coordinated actions of GADD34/PP1 and SNAT2. Fragmented Golgi has been shown to have a negative impact on trafficking of some proteins, though a stimulatory effect on trafficking of others (Xiang et al., 2013). It was previously shown that the GADD34 interactome includes cytoskeletal elements, as well as KIF3A, a motor protein driving intracellular, microtubule-based anterograde transport (Chambers et al., 2015; Hasegawa et al., 2000). First we tested whether this association is maintained in hyperosmolar conditions. We used cornea epithelial cells transiently expressing a FLAG-tagged GADD34 protein and attempted to co-immunoprecipitate α-tubulin and KIF3A, as well as the known interactors eIF2α and the subunit of the PP1 phosphatase PP1. All four proteins were found to interact with GADD34 in control and stress conditions when cytoplasmic protein GAPDH was absent in the immunoprecipitations, which ensured specificity of immunoprecipitations (Fig. S4A). At the same time, inhibition of GADD34/PP1 by Sephin 1 did not change the interaction of GADD34 with α-tubulin, KIF3A and eIF2α (Fig. S4A).

We next tested the effect of nocodazole (Noc), a microtubule polymerization inhibitor, on the subcellular distribution of SNAT2 during hyperosmotic stress. In the presence of Noc throughout the entire treatment with hyperosmotic media (5h), we did not observe SNAT2 localization to the PM, but instead an intracellular punctate pattern (Fig. S4B). To further

explore the action of Noc on SNAT2 maturation we treated cells with this inhibitor for the last 2h of a 5h stress treatment. This strategy allows for both accumulation of SNAT2 protein and observation of its continuing maturation in the presence of the inhibitor. Inhibition of microtubule polymerization resulted in accumulation of the immature form of SNAT2 (Fig. S4C) and subsequent decrease of transporter activity (Fig. S4D). These data suggested decreased maturation and delivery of SNAT2 to the PM after disruption of the microtubule network. Noc (last 2h of treatment with stress) induced disassembly of microtubules and diffused staining of monomeric α-tubulin (Fig. S4E). At the same time, the Golgi apparatus was fragmented as shown by the distribution of the *cis*-Golgi marker GM130 (Fig. S4E).

We also used a genetic model of Golgi fragmentation by depletion of the Golgi Reassembly Stacking Protein 2 (GORASP2) using shRNA. GORASP2 establishes the stacked morphology of the Golgi, and its depletion was previously shown to induce Golgi fragmentation (Xiang et al., 2013). GORASP2 silencing resulted in lower levels of SNAT2 protein both in the basal condition and upon exposure to mild hyperosmotic stress (Fig. 4A). These data suggest that fragmentation of Golgi has a negative effect on SNAT2 maturation. Next we tested if increased Golgi fragmentation due to stress intensity would have similar effects on SNAT2 maturation. Cells exposed to mild stress of 500 mOsm followed with a switch to 600 mOsm media showed an increase in the percent of cells with fragmented Golgi (Fig. 4B). We then used this experimental paradigm to further examine the maturation of SNAT2. Cells were exposed to mild hyperosmotic stress for 3h, which caused the accumulation of both, mature and immature SNAT2 (Fig 4C, immature SNAT2 is shown). Cells were subsequently incubated in 500 or 600 mOsm media for an additional 2h in the presence of cyclohexmide (CX) to prevent *de novo* SNAT2 protein synthesis during this time frame. In 500 mOsm media, the immature form diminished after 30 min. In contrast, a shift to 600 mOsm media delayed the anterograde trafficking of the immature form and the levels of the mature SNAT2 did not change (Fig. 4C,D, S4F). These data strongly support the conclusion that maturation and delivery of SNAT2 to the PM requires Golgi integrity, and are negatively correlated with the degree of Golgi fragmentation and the intensity of stress.

To demonstrate the contribution of GADD34/PP1 to SNAT2 maturation during mild stress, we hypothesized that GADD34/PP1 inhibition after 3h of exposure of cells to mild stress would result in immature transporter accumulation. In this condition, inhibition of GADD34/PP1 by Sal003 induced eIF2α phosphorylation and accumulation of immature SNAT2 (Fig. 4E,F). We then incubated cells with hyperosmotic media in the presence of CX with or without Sal003, and studied the trafficking of immature SNAT2 protein (Fig. 4G,H). The existing immature SNAT2 declined during subsequent incubation in the absence of Sal003, consistent with its export from the ER and processing in the Golgi. Significantly, the inhibition of GADD34/PP1 by Sal003 delayed the loss of immature SNAT2, consistent with decreased conversion to the mature form by glycosylation in the Golgi.

GADD34/PP1 inhibition delays trafficking of SNAT2 from cis- to trans-Golgi

Immunofluorescent staining of SNAT2 clearly demonstrated a very strong cisternae-like pattern of SNAT2 subcellular distribution, which suggests that a significant amount of the

protein in the cell is localized to the Golgi complex at any given time (Fig. 1G), with or without GADD34.

To study the movement of SNAT2 through Golgi and the contribution of GADD34 to this process, cells were exposed to mild hyperosmotic stress for 5h with or without the addition of Sal003, and SNAT2 intra-Golgi distribution was analyzed. GM130 was used as a *cis*-Golgi marker (labeled with red color), TGN46 was used as a *trans*-Golgi marker (labeled with blue color), and SNAT2 was labeled using green color (Fig. 5A). We adopted the linescan methodology for intra-Golgi distribution of proteins, which was originally developed to analyze the localization of resident Golgi proteins (Dejgaard et al., 2007). This approach is based on visual separation between *cis*- and *trans*-Golgi ribbons in order to assign the protein of interest to either compartment. In cells experiencing hyperosmotic stress, the peak of SNAT2 signal spreads between peaks of *cis*- and *trans*- Golgi (GM130 and TGN46)(Fig. 5B), which would correspond to the trafficking of “cargo” protein through different Golgi cisterns, rather than localization of SNAT2 within one particular compartment within Golgi. Addition of Sal003 resulted in a shift of a SNAT2 peak towards *cis*-Golgi, with no overlap with the *trans*-Golgi marker TGN46 (Fig. 5A,B). This suggests that Sal003 resulted in delayed processing of SNAT2 within the Golgi structures.

During the analysis, we noted that in corneal epithelial cells experiencing hyperosmotic stress for 5h, the Golgi structure is very compact, which is shown as almost a complete overlap of red and blue signal (Fig. 5C). In the presence of Sal003 separation of *cis*- and *trans*- Golgi markers was clearly visible as shown in Fig. 5C (right panel), with a significant amount of TGN46 (blue signal) not being masked by GM130 (red). The same changes from compacted Golgi structure to visibly separated *cis*- and *trans*- Golgi compartments were obtained using a different *trans*-Golgi marker protein, the UDP-galactose transporter, SLC35A2 (Song, 2013). This effect of Sal003 is very similar to the well described action of Noc, which increases separation between *cis*- and *trans*-Golgi compartments in Hela cells (Dejgaard et al., 2007), due to the Noc effect on microtubules. Indeed, Noc addition resulted in increased distance between *cis*- and *trans*-Golgi markers in corneal epithelial cells (Fig. S5A). Importantly, not only the addition of Sal003 but also expression of shRNA targeting GADD34, led to the separation between *cis*- (GM130) and *trans*-Golgi (SLC35A2) markers (Fig. S5A–C). Therefore, inactivation of GADD34/PP1 by Sal003 or by shRNA resulted in Golgi fragmentation, accompanied by a high degree of separation between *cis*- and *trans*-Golgi regions.

Analysis of SNAT2 intra-Golgi distribution presented in Fig 5D suggested that the GADD34 absence leads to decreased SNAT2 trafficking from *cis*- to *trans*- Golgi. The percentage of the area stained by SNAT2 (green color) and GM130 overlapping within single planes was calculated. In stressed cells, the steady state distribution of SNAT2 was wider than that of GM130. There was only partial co-localization between these two proteins, and a significant portion of the SNAT2 signal was localized in the close proximity with (but without exclusive overlap to) GM130 (Fig. 5E–G). This is explained by SNAT2 transitioning through *cis*- and *trans*-Golgi. Addition of Sal003 resulted in significant increase in co-localization of SNAT2 with GM130 (Fig. 5E–G). We have additionally confirmed those results in corneal cells expressing shRNA against GADD34. In cells with decreased levels of GADD34, exposed to

hyperosmotic media, colocalization of SNAT2 with the *cis*-Golgi marker was higher as compared to shCon (Fig. 5G, S5D). Therefore, inactivation of GADD34 genetically or pharmacologically leads to retention of SNAT2 in the *cis*-Golgi compartment.

In conclusion, adaptation to mild hyperosmotic stress is characterized by fast processing and trafficking of SNAT2 through the Golgi complex (from *cis*- to *trans*-Golgi). The activity of GADD34/PP1 is required for maintenance of Golgi integrity during stress, which promotes maturation of SNAT2 during processing and trafficking to the PM. In the absence of functional GADD34/PP1, Golgi morphology is not recovering from stress induced fragmentation, resulting in increased separation of *cis*- *trans*- compartments, and trapping of SNAT2 in the *cis*-Golgi, with significant inhibition of its membrane localization.

The function of GADD34 on SNAT2 maturation is independent of the eIF2α phosphorylation status

A well-studied function of the GADD34/PP1 phosphatase is the dephosphorylation of eIF2α and subsequent regulation of protein synthesis rates (Novoa et al., 2001). The studies with ISRIB (Fig. 3F) suggested that the GADD34/PP1 effects on maturation and trafficking of SNAT2 during hyperosmotic stress, are independent of its target, eIF2α-P. We further tested this idea in MEFs with a homozygous mutation of the eIF2α phosphorylation site (S51A). We have published previously (Krokowski et al., 2015) that hyperosmotic stress induced SNAT2 and GADD34 in MEFs. Similar to WT cells, GADD34 and SNAT2 were induced in S51A MEFs (Fig. 6A, S6A). SNAT2 protein localized in the membranes (Fig. 6B; S6B) and was functional as demonstrated by the increased uptake of its substrate MeAIB (Fig. 6C). Similarly to corneal epithelial cells and WT MEFs (Krokowski et al., 2015), induction of transporter activity was attenuated when GADD34/PP1 was inhibited without a decrease in SNAT2 mRNA levels (Fig. 6C,D). To demonstrate that the effects of GADD34/PP1 activity on SNAT2-mediated transport is not due to changes in SNAT2 protein levels, we compared the levels of an N-terminal fragment of the SNAT2 protein in cell extracts treated with *o*-iodoxybenzoic acid (IBX) which breaks polypeptide chains on tryptophan residues. This approach releases a ~20 kDa (1–190 aa) fragment at the N-terminal of SNAT2 which does not contain glycosylated asparagine residues (Fig. S6C). This fragment migrates as a single band in SDS-PAGE and is recognized by the antibody directed against SNAT2, thus allowing a direct comparison of SNAT2 protein levels between different samples. As expected, N-terminal SNAT2 protein fragment was induced by hyperosmotic stress (Fig. S6D). Neither Sal003 nor Sephin 1 decreased this induction (Fig. S6D). These data support the conclusion that the action of GADD34/PP1 on SNAT2 maturation is independent of SNAT2 gene transcription or SNAT2 mRNA translation (Krokowski et al., 2015).

Inhibition of GADD34/PP1 in S51A MEFs resulted in the accumulation of the immature SNAT2 protein corresponding to the ER glycosylated form, similar to the observations in corneal epithelial cells (Fig. 6E). Furthermore, genetic depletion of GADD34 decreased the levels of the mature SNAT2 protein (Fig. 6F). We confirmed next that, similar to corneal epithelial cells, both hyperosmotic stress and inhibition of GADD34/PP1 induced Golgi fragmentation (Fig. 6G, S6E). Furthermore, the effect of GADD34 inhibitors is specific to their target protein, as GADD34/PP1 deficient MEFs ($GADD3^{\Delta C/\Delta C}$) did not induce Golgi

fragmentation when treated with Sephin 1 (Fig. S7A). GADD3$^{\Delta C/\Delta C}$ MEFs express a truncated GADD34 protein which is unable to interact with the PP1 holoenzyme (Novoa et al., 2003). As expected Sal003 caused some increase in Golgi fragmentation most likely due to its inhibitory effect on CReP (Fig. S7A). We next showed that hyperosmotic stress induced significant changes in the microtubule network in S51A MEFs. Short exposure to mild stress (500 mOsm, 30 min) resulted in the detachment of the microtubular structures from the PM, which was shown by the actin-positive peripheral zones without α-tubulin signal (Fig. 6H). As adaptation progressed (5h of stress) the microtubule network was restored, and the cytoplasm was uniformly labeled with both F-actin- and α-tubulin- positive structures (Fig. 6H). The presence of Sephin 1 in control or hyperosmotic media resulted in the retraction of microtubules from the PM, with minor changes in the actin network (Fig. 6H). These data further support the conclusion that changes in the dynamics of tubulin polymerization can be the cause of Golgi fragmentation in response to GADD34/PP1 inhibition. To further support this hypothesis we treated stressed cells with Noc (Minin, 1997). Noc had effects similar to the GADD34/PP1 inhibitor, indicated by the accumulation of immature SNAT2 (Fig. 6I). Immunofluorescence staining revealed that the expected disassembly of microtubules was also accompanied with fragmentation of Golgi (Fig. 6J).

In summary, inhibition of GADD34/PP1 induced changes in the microtubule network and increased Golgi fragmentation in a manner independent of its functions on eIF2α-P. Furthermore, the decreased SNAT2 activity upon GADD34/PP1 inhibition is the result of inhibited SNAT2 protein processing and maturation, resulting in accumulation of the immature ER-glycosylated form. This function of GADD34/PP1 is independent of the well-established actions of the phosphatase in regulation of protein synthesis during stress.

Genetic depletion of active GADD34/PP1 attenuates GPI-EGFP trafficking from the ER to PM during hyperosmotic stress

To test if the GADD34 effects on Golgi integrity and protein trafficking are extended to other than SNAT2 cargo proteins during hyperosmotic stress, we used the RUSH technology. Two fusion proteins were introduced into the cells: the ER-anchor, KDEL, fused to streptavidin and the cargo reporter GPI-EGFP fused to the streptavidin-binding peptide (Boncompain et al., 2012). The GPI protein was used as a cargo reporter, because it undergoes posttranslational modifications in the Golgi apparatus (Kinoshita et al., 2013). The KDEL-streptavidin anchor ensures ER localization of the GPI-EGFP. Biotin addition disrupts anchor-cargo interaction and induces a synchronous release of the GPI-EGFP from the ER. GPI-EGFP release was tested in WT and GADD34 $^{\Delta C/\Delta C}$ MEFs subjected to hyperosmotic stress. Prior to the biotin addition at 0 time point in MEFs transfected with the plasmid expressing both proteins, GPI-EGFP showed uniform distribution with characteristics for an ER reticular pattern (Fig. 7A). Upon biotin addition, GPI-EGFP was released from the ER and trafficked to the Golgi apparatus (center-located structure), from where it subsequently reached the PM (Fig. 7A).

A time-course performed in WT MEFs determined that after 40 minutes of biotin treatment the majority of the GPI-EGFP localizes to Golgi-like structures in over 90% of the cells; while after 60 minutes GPI-EGFP clears from the Golgi and reaches PM in over 75 % of the

cells (Fig. S7B). Therefore 40 minutes is an appropriate time point to analyze trafficking of GPI-EGFP to the Golgi, and 60 minutes is a proper time point to analyze trafficking from Golgi to PM.

Next the effect of hyperosmolar stress on trafficking of GPI-EGFP was compared in WT and GADD34 $^{\Delta C/\Delta C}$ MEFs. 40 minutes post-biotin addition, the majority of the cells demonstrated that GPI-EGFP reached the central Golgi-like structure as well as some vesicular intracellular compartments. No significant differences between WT and GADD34$^{\Delta C/\Delta C}$ cells (Fig. S7B; compare total number of cells with GPI-EGFP in Golgi) were found. Therefore trafficking of GPI-EGFP to Golgi does not depend on functional GADD34. 60 minutes post-biotin addition, as expected from the time course in unstressed cells, GPI-EGFP cleared from the Golgi and reached the PM in 75% of the cells in WT MEFs (Fig. 7B). During hyperosmotic stress clearance of GPI-EGFP from the Golgi-like structures and delivery to PM (cells as in Fig. 7A, PM, no visible central Golgi-like structure) was significantly slower in GADD34$^{\Delta C/\Delta C}$ MEFs, (only 49% of the cells cleared GPI-EGFP from Golgi) (Fig. 7, S7B). Moreover, Golgi trapping and slow PM delivery can be seen in GADD34$^{\Delta C/\Delta C}$ MEFs in both control and hyperosmotic stress conditions, the effect being more prominent in cells exposed to stress (Fig. 7B, S7B). GADD34 regulates trafficking and maturation of proteins modified through the Golgi apparatus, especially in cells exposed to stress.

Discussion

We report here the response of cultured human corneal epithelial cells to increased osmolarity generated by sodium chloride, a physiologically-relevant solute of the tear film (Stahl et al., 2012). Mild stress (500 mOsm) triggered a osmoadaptive program that involved the actions of the GADD34/PP1 phosphatase and the amino acid transporter SNAT2, which facilitates the uptake of compatible osmolytes. This osmoadaptation mechanism was shown to consist of (i) mild stress-induced gene expression of both SNAT2 and the regulatory subunit of the PP1 phosphatase GADD34, and (ii) post-translational processing of SNAT2 via the Golgi apparatus and subsequent localization to the PM, via the positive actions of the GADD34/PP1 on attenuating stress-induced Golgi fragmentation. In contrast, the lack of SNAT2 and GADD34 induction during severe hyperosmotic stress (600 mOsm) abolished osmoadaptation.

Adaptation to increased extracellular osmolarity has been extensively studied at the level of transcriptional control (Burg et al., 2007). We show here that GADD34/PP1 is required for the adaptive recovery of Golgi integrity in response to mild hyperosmotic stress. In agreement with the adaptive role of GADD34 in protein trafficking, we have also shown that GADD34/PP1 inhibition does not attenuate the increased transcription (Krokowski et al., 2015) or stress-insensitive translation of SNAT2 mRNA (Gaccioli et al., 2006). Instead, it inhibits SNAT2 protein maturation in the Golgi. SNAT2 as a membrane protein undergoes numerous maturation steps on its way from the ER through the Golgi to the cell surface. The glycosylation of two asparagine residues of the SNAT2 protein in the ER is followed by extensive modification in the Golgi (Broer, 2014). Inactivation of GADD34 caused

accumulation of the ER-glycosylated form in *cis*-Golgi and a decrease in the levels of the mature transporter protein on the PM.

The exact mechanism via which GADD34/PP1 activity assists SNAT2 protein maturation is not known. However, our data suggest that during hyperosmotic stress the induction of GADD34 associates with the rescue from stress-induced changes in tubulin polymerization and Golgi fragmentation. Recovery from these changes promotes SNAT2 maturation. Here we observed that the hyperosmotic stress-induced initial microtubule detachment from the PM was followed by restoration of the microtubule network. This reversal correlated with accumulation of GADD34 protein levels. Inhibition of GADD34/PP1 showed (i) a retraction of the microtubule network from the cell periphery, (ii) fragmentation and a spatial separation between the *cis*- and *trans*- cisternae of the Golgi apparatus, (iii) decreased accumulation on the PM of Golgi-processed SNAT2, and (iv) decreased presence of microtubule threads extending to the cell periphery. Moreover, fragmentation of Golgi and separation of *cis*- *trans*- cisternae upon GADD34/PP1 inhibition or depletion are strikingly similar to the effects of Noc, an inhibitor of microtubule polymerization (Dejgaard et al., 2007; Sandoval et al., 1984). Hyperosmotic stress has a pronounced effect on the microtubule network, with transient depolymerization upon exposure to stress and reassembly during adaptation (Nunes et al., 2013). Hyperosmolarity has been shown to induce a series of phosphorylation events, including modification of α-tubulin and stathmin, proteins involved in cytoskeletal organization (Ban et al., 2013; Yip et al., 2014). It is therefore possible that GADD34/PP1 modulates phosphorylation events on unknown target(s) that are involved in microtubule organization during hyperosmotic stress. In support of this idea, numerous cytoskeletal elements, including α- and β-tubulins (Chambers et al., 2015) as well as a microtubule-based anterograde intracellular transport motor protein of the kinesin family (Hasegawa et al., 2000) were found as part of the GADD34 interactome. Future studies will determine how GADD34/PP1 regulates cytoskeleton dynamics during hyperosmotic stress, and by doing so promotes Golgi integrity and insures successful onset of osmoadaptation.

Our finding of GADD34/PP1 promoting SNAT2 *cis*- to *trans*- Golgi trafficking may also imply a direct action(s) of the phosphatase on the Golgi apparatus, independently of the microtubule network. Golgi fragmentation is a regulated process. For example, the Golgi undergoes extensive transient fragmentation at the onset of mitosis. Several protein kinases which are activated by hyperosmotic stress, are also are involved in the regulation of Golgi integrity during cell division. Because phosphorylation is involved and global inhibition of phosphatases has been shown to induce Golgi fragmentation (Lucocq et al., 1991), it is possible that GADD34 is required to reverse stress-induced changes in the Golgi apparatus. This would involve unknown target(s) of the GADD34/PP1 phosphatase. The subcellular localization of GADD34 supports this hypothesis. In stressed cells GADD34 is recruited to intracellular membrane compartments via its N-terminal domain (Brush et al., 2003), which can assist the proximity of the phosphatase complex with proteins involved in Golgi integrity.

The uptake of amino acids during hyperosmotic stress is known to be an important part of the RVI. Of the ten most abundant amino acids in tears, five are substrates for the

concentrative uptake by SNAT2 (Nakatsukasa et al., 2011). In addition, amino acids, including the SNAT2 substrates Gly and Pro, have been used in teardrops to treat dysfunctional tear production (Aragona et al., 2013). Our research provides a rationale for using amino acids as a component of tear substitutes and offers an interesting opportunity to use amino acids and non-metabolized amino acid analogs as a potential pharmacological intervention to increase adaptation as a treatment for dry eye syndrome. In addition to the benefits of our studies for ocular diseases, our finding of the GADD34/PP1 functions in Golgi integrity reveal an unrecognized molecular mechanism that can control the sensitivity of cells to stress-induced Golgi fragmentation, and therefore influence development of diseases in a cell-type specific manner.

Materials and methods

Cells

Immortalized human corneal epithelial cells (10.014 pRSV-T) were grown in Keratinocyte-SFM (ThermoFisher Scientific) with 5 ng/ml epidermal growth factor, 0.05 mg/ml bovine pituitary extract, 0.005 mg/ml insulin and 500 ng/ml hydrocortisone on dishes coated with fibronectin, type I bovine collagen, and BSA. Mouse embryonic fibroblasts were grown in DMEM supplemented with 10% FBS, 2mM L-glutamine, 100 units/ml penicillin and 100 μg/ml streptomycin. Cells were kept in a humidified atmosphere of 5% CO_2 at 37°C.

Viral particles, and chemicals

Propagation of lentiviral particles expressing shRNA against human SNAT2, GORASP2 and human and mouse GADD34 (TRCN0000020239, TRCN0000278406, TRCN0000003041 and TRCN0000353349, respectively; Sigma-Aldrich) or empty vector (pLKO.1) was performed in HEK293T cells. The osmolarity of media was increased by addition of NaCl for corneal epithelial cells or sorbitol for MEFs. The following reagents were purchased from commercial vendors: Sal003, nocodazole, ISRIB, brefeldin A and golgicide A (Tocris); cycloheximide, MG132, guanabenz and tunicamycin (Sigma-Aldrich). Sephin 1 was a generous gift from Anne Bertolotti (University of Cambridge, UK).

SNAT2 amino acid transporter activity

SNAT2-mediated amino acid uptake (System A activity) was measured as previously described (Krokowski et al., 2015). Cells were grown in 24-well plates and the uptake of ^{14}C-MeAIB was measured in Earle's balanced salt solution in the presence of sodium ions for 3 min at 37°C. Cells were washed 2X with ice cold PBS to remove MeAIB, and the intracellular amino acid pool was extracted with absolute ethanol. Radioactivity was measured by scintillation counter and normalized to protein content.

Statistical methods

To evaluate statistical significance one-way ANOVA or two-way ANOVA with post-hoc Benferroni test was used. Analysis was conducted using Origin software. A *p*-value of less than 0.05 was considered statistically significant. * - $p<0.05$; ** - $p<0.01$ and *** - $p<0.001$.

Supplementary Material

Refer to Web version on PubMed Central for supplementary material.

Acknowledgments

This work was supported by National Institutes of Health Grants R37-DK60596, R01-DK53307 (to M.H.), R01GM092960, U54GM105814 (to B.S), VSRC Core Grant (P30-EY11373) and American Diabetes Association postdoctoral fellowship to X.G. (1-17-PDF-129). The content is solely the responsibility of the authors and does not necessarily represent the official views of the National Institutes of Health. Thanks also to Kenneth Farabaugh for editing this manuscript.

References

Allan VJ, Thompson HM, McNiven MA. Motoring around the Golgi. Nature cell biology. 2002; 4:E236–242. [PubMed: 12360306]

Aragona P, Rania L, Roszkowska AM, Spinella R, Postorino E, Puzzolo D, Micali A. Effects of amino acids enriched tears substitutes on the cornea of patients with dysfunctional tear syndrome. Acta ophthalmologica. 2013; 91:e437–444. [PubMed: 23617248]

Ban Y, Kobayashi Y, Hara T, Hamada T, Hashimoto T, Takeda S, Hattori T. alpha-Tubulin is Rapidly Phosphorylated in Response to Hyperosmotic Stress in Rice and Arabidopsis. Plant Cell Physiol. 2013; 54:848–858. [PubMed: 23628996]

Bevilacqua E, Bussolati O, Dall'Asta V, Gaccioli F, Sala R, Gazzola GC, Franchi-Gazzola R. SNAT2 silencing prevents the osmotic induction of transport system A and hinders cell recovery from hypertonic stress. FEBS letters. 2005; 579:3376–3380. [PubMed: 15922329]

Bevilacqua E, Wang X, Majumder M, Gaccioli F, Yuan CL, Wang C, Zhu X, Jordan LE, Scheuner D, Kaufman RJ, et al. eIF2alpha phosphorylation tips the balance to apoptosis during osmotic stress. J Biol Chem. 2010; 285:17098–17111. [PubMed: 20338999]

Bhavsar AS, Bhavsar SG, Jain SM. A review on recent advances in dry eye: Pathogenesis and management. Oman J Ophthalmol. 2011; 4:50–56. [PubMed: 21897618]

Boncompain G, Divoux S, Gareil N, de Forges H, Lescure A, Latreche L, Mercanti V, Jollivet F, Raposo G, Perez F. Synchronization of secretory protein traffic in populations of cells. Nature methods. 2012; 9:493–498. [PubMed: 22406856]

Boyce M, Bryant KF, Jousse C, Long K, Harding HP, Scheuner D, Kaufman RJ, Ma D, Coen DM, Ron D, et al. A selective inhibitor of eIF2alpha dephosphorylation protects cells from ER stress. Science. 2005; 307:935–939. [PubMed: 15705855]

Brocker C, Thompson DC, Vasiliou V. The role of hyperosmotic stress in inflammation and disease. Biomol Concepts. 2012; 3:345–364. [PubMed: 22977648]

Broer S. The SLC38 family of sodium-amino acid co-transporters. Pflugers Arch. 2014; 466:155–172. [PubMed: 24193407]

Brush MH, Weiser DC, Shenolikar S. Growth arrest and DNA damage-inducible protein GADD34 targets protein phosphatase 1 alpha to the endoplasmic reticulum and promotes dephosphorylation of the alpha subunit of eukaryotic translation initiation factor 2. Molecular and cellular biology. 2003; 23:1292–1303. [PubMed: 12556489]

Burg MB, Ferraris JD, Dmitrieva NI. Cellular response to hyperosmotic stresses. Physiol Rev. 2007; 87:1441–1474. [PubMed: 17928589]

Carrara M, Sigurdardottir A, Bertolotti A. Decoding the selectivity of eIF2alpha holophosphatases and PPP1R15A inhibitors. Nature structural & molecular biology. 2017

Chambers JE, Dalton LE, Clarke HJ, Malzer E, Dominicus CS, Patel V, Moorhead G, Ron D, Marciniak SJ. Actin dynamics tune the integrated stress response by regulating eukaryotic initiation factor 2alpha dephosphorylation. eLife. 2015; 4

Choy MS, Yusoff P, Lee IC, Newton JC, Goh CW, Page R, Shenolikar S, Peti W. Structural and Functional Analysis of the GADD34:PP1 eIF2 alpha Phosphatase. Cell Rep. 2015; 11:1885–1891. [PubMed: 26095357]

Czech A, Wende S, Morl M, Pan T, Ignatova Z. Reversible and rapid transfer-RNA deactivation as a mechanism of translational repression in stress. PLoS genetics. 2013; 9:e1003767. [PubMed: 24009533]

Dall'Asta V, Rossi PA, Bussolati O, Gazzola GC. Response of human fibroblasts to hypertonic stress. Cell shrinkage is counteracted by an enhanced active transport of neutral amino acids. J Biol Chem. 1994; 269:10485–10491. [PubMed: 8144632]

Das I, Krzyzosiak A, Schneider K, Wrabetz L, D'Antonio M, Barry N, Sigurdardottir A, Bertolotti A. Preventing proteostasis diseases by selective inhibition of a phosphatase regulatory subunit. Science. 2015; 348:239–242. [PubMed: 25859045]

Dejgaard SY, Murshid A, Dee KM, Presley JF. Confocal microscopy-based linescan methodologies for intra-golgi localization of proteins. J Histochem Cytochem. 2007; 55:709–719. [PubMed: 17341478]

Di Prisco GV, Huang W, Buffington SA, Hsu CC, Bonnen PE, Placzek AN, Sidrauski C, Krnjevic K, Kaufman RJ, Walter P, et al. Translational control of mGluR-dependent long-term depression and object-place learning by eIF2alpha. Nature neuroscience. 2014; 17:1073–1082. [PubMed: 24974795]

Eveloff JL, Warnock DG. Activation of ion transport systems during cell volume regulation. The American journal of physiology. 1987; 252:F1–10. [PubMed: 3544865]

Franchi-Gazzola R, Dall'Asta V, Sala R, Visigalli R, Bevilacqua E, Gaccioli F, Gazzola GC, Bussolati O. The role of the neutral amino acid transporter SNAT2 in cell volume regulation. Acta Physiol (Oxf). 2006; 187:273–283. [PubMed: 16734764]

Freeze HH, Kranz C. Endoglycosidase and glycoamidase release of N-linked glycans. Current protocols in molecular biology. 2010; Chapter 17(Unit 17):13A.

Gaccioli F, Huang CC, Wang C, Bevilacqua E, Franchi-Gazzola R, Gazzola GC, Bussolati O, Snider MD, Hatzoglou M. Amino acid starvation induces the SNAT2 neutral amino acid transporter by a mechanism that involves eukaryotic initiation factor 2alpha phosphorylation and cap-independent translation. J Biol Chem. 2006; 281:17929–17940. [PubMed: 16621798]

Grueb M, Bartz-Schmidt KU, Rohrbach JM. Adrenergic regulation of cAMP/protein kinase A pathway in corneal epithelium and endothelium. Ophthalmic Res. 2008; 40:322–328. [PubMed: 18688175]

Hasegawa T, Yagi A, Isobe K. Interaction between GADD34 and kinesin superfamily, KIF3A. Biochem Bioph Res Co. 2000; 267:593–596.

Hetz C, Chevet E, Harding HP. Targeting the unfolded protein response in disease. Nat Rev Drug Discov. 2013; 12:703–719. [PubMed: 23989796]

Hetz C, Chevet E, Oakes SA. Proteostasis control by the unfolded protein response. Nature cell biology. 2015; 17:829–838. [PubMed: 26123108]

Kinoshita T, Maeda Y, Fujita M. Transport of glycosylphosphatidylinositol-anchored proteins from the endoplasmic reticulum. Biochimica et biophysica acta. 2013; 1833:2473–2478. [PubMed: 23380706]

Krokowski D, Jobava R, Guan BJ, Farabaugh K, Wu J, Majumder M, Bianchi MG, Snider MD, Bussolati O, Hatzoglou M. Coordinated Regulation of the Neutral Amino Acid Transporter SNAT2 and the Protein Phosphatase Subunit GADD34 Promotes Adaptation to Increased Extracellular Osmolarity. J Biol Chem. 2015; 290:17822–17837. [PubMed: 26041779]

Lam H, Bleiden L, De Paiva CS, Farley W, Stern ME, Pflugfelder SC. Tear Cytokine Profiles in Dysfunctional Tear Syndrome. Am J Ophthalmol. 2009; 147:198–205. [PubMed: 18992869]

Lang F, Busch GL, Ritter M, Volkl H, Waldegger S, Gulbins E, Haussinger D. Functional significance of cell volume regulatory mechanisms. Physiol Rev. 1998; 78:247–306. [PubMed: 9457175]

Lin Z, Liu X, Zhou T, Wang Y, Bai L, He H, Liu Z. A mouse dry eye model induced by topical administration of benzalkonium chloride. Mol Vis. 2011; 17:257–264. [PubMed: 21283525]

Lucocq J, Warren G, Pryde J. Okadaic acid induces Golgi apparatus fragmentation and arrest of intracellular transport. J Cell Sci. 1991; 100(Pt 4):753–759. [PubMed: 1667660]

Luo L, Li DQ, Pflugfelder SC. Hyperosmolarity-induced apoptosis in human corneal epithelial cells is mediated by cytochrome c and MAPK pathways. Cornea. 2007; 26:452–460. [PubMed: 17457195]

Minin AA. Dispersal of Golgi apparatus in nocodazole-treated fibroblasts is a kinesin-driven process. J Cell Sci. 1997; 110:2495–2505. [PubMed: 9410887]

Nakatsukasa M, Sotozono C, Shimbo K, Ono N, Miyano H, Okano A, Hamuro J, Kinoshita S. Amino Acid profiles in human tear fluids analyzed by high-performance liquid chromatography and electrospray ionization tandem mass spectrometry. Am J Ophthalmol. 2011; 151:799–808. e791. [PubMed: 21310375]

Novoa I, Zeng H, Harding HP, Ron D. Feedback inhibition of the unfolded protein response by GADD34-mediated dephosphorylation of eIF2alpha. J Cell Biol. 2001; 153:1011–1022. [PubMed: 11381086]

Novoa I, Zhang Y, Zeng H, Jungreis R, Harding HP, Ron D. Stress-induced gene expression requires programmed recovery from translational repression. The EMBO journal. 2003; 22:1180–1187. [PubMed: 12606582]

Nunes P, Ernandez T, Roth I, Qiao XM, Strebel D, Bouley R, Charollais A, Ramadori P, Foti M, Meda P, et al. Hypertonic stress promotes autophagy and microtubule-dependent autophagosomal clusters. Autophagy. 2013; 9:550–567. [PubMed: 23380587]

Pedersen SF, Darborg BV, Rasmussen M, Nylandsted J, Hoffmann EK. The Na+/H+ exchanger, NHE1, differentially regulates mitogen-activated protein kinase subfamilies after osmotic shrinkage in Ehrlich Lettre Ascites cells. Cell Physiol Biochem. 2007; 20:735–750. [PubMed: 17982256]

Ruggiano A, Foresti O, Carvalho P. Quality control: ER-associated degradation: protein quality control and beyond. J Cell Biol. 2014; 204:869–879. [PubMed: 24637321]

Saikia M, Jobava R, Parisien M, Putnam A, Krokowski D, Gao XH, Guan BJ, Yuan Y, Jankowsky E, Feng Z, et al. Angiogenin-cleaved tRNA halves interact with cytochrome c, protecting cells from apoptosis during osmotic stress. Molecular and cellular biology. 2014; 34:2450–2463. [PubMed: 24752898]

Sanchez JC, Wilkins RJ. Changes in intracellular calcium concentration in response to hypertonicity in bovine articular chondrocytes. Comp Biochem Physiol A Mol Integr Physiol. 2004; 137:173–182. [PubMed: 14720602]

Sandoval IV, Bonifacino JS, Klausner RD, Henkart M, Wehland J. Role of Microtubules in the Organization and Localization of the Golgi-Apparatus. J Cell Biol. 1984; 99:S113–S118.

Sidrauski C, McGeachy AM, Ingolia NT, Walter P. The small molecule ISRIB reverses the effects of eIF2alpha phosphorylation on translation and stress granule assembly. eLife. 2015; 4

Song Z. Roles of the nucleotide sugar transporters (SLC35 family) in health and disease. Molecular aspects of medicine. 2013; 34:590–600. [PubMed: 23506892]

Stahl U, Willcox M, Stapleton F. Osmolality and tear film dynamics. Clin Exp Optom. 2012; 95:3–11. [PubMed: 22022802]

Tsaytler P, Harding HP, Ron D, Bertolotti A. Selective inhibition of a regulatory subunit of protein phosphatase 1 restores proteostasis. Science. 2011; 332:91–94. [PubMed: 21385720]

Xiang Y, Zhang X, Nix DB, Katoh T, Aoki K, Tiemeyer M, Wang Y. Regulation of protein glycosylation and sorting by the Golgi matrix proteins GRASP55/65. Nature communications. 2013; 4:1659.

Yamamoto M, Chen MZ, Wang YJ, Sun HQ, Wei Y, Martinez M, Yin HL. Hypertonic stress increases phosphatidylinositol 4,5-bisphosphate levels by activating PIP5KIbeta. J Biol Chem. 2006; 281:32630–32638. [PubMed: 16943196]

Yeh S, Song XJ, Farley W, Li DQ, Stern ME, Pflugfelder SC. Apoptosis of ocular surface cells in experimentally induced dry eye. Investigative ophthalmology & visual science. 2003; 44:124–129. [PubMed: 12506064]

Yip YY, Yeap YYC, Bogoyevitch MA, Ng DCH. cAMP-dependent Protein Kinase and c-Jun N-terminal Kinase Mediate Stathmin Phosphorylation for the Maintenance of Interphase Microtubules during Osmotic Stress. J Biol Chem. 2014; 289:2157–2169. [PubMed: 24302736]

Highlights

- GADD34, a stress-inducible subunit of the PP1 phosphatase, promotes osmoadaptation
- The functions of GADD34 in osmoadaptation are independent of its substrate eIF2α-P
- GADD34/PP1 facilitates *cis*- to *trans*- Golgi SNAT2 protein trafficking
- Pharmacologic and genetic inhibition of GADD34/PP1 induce Golgi fragmentation

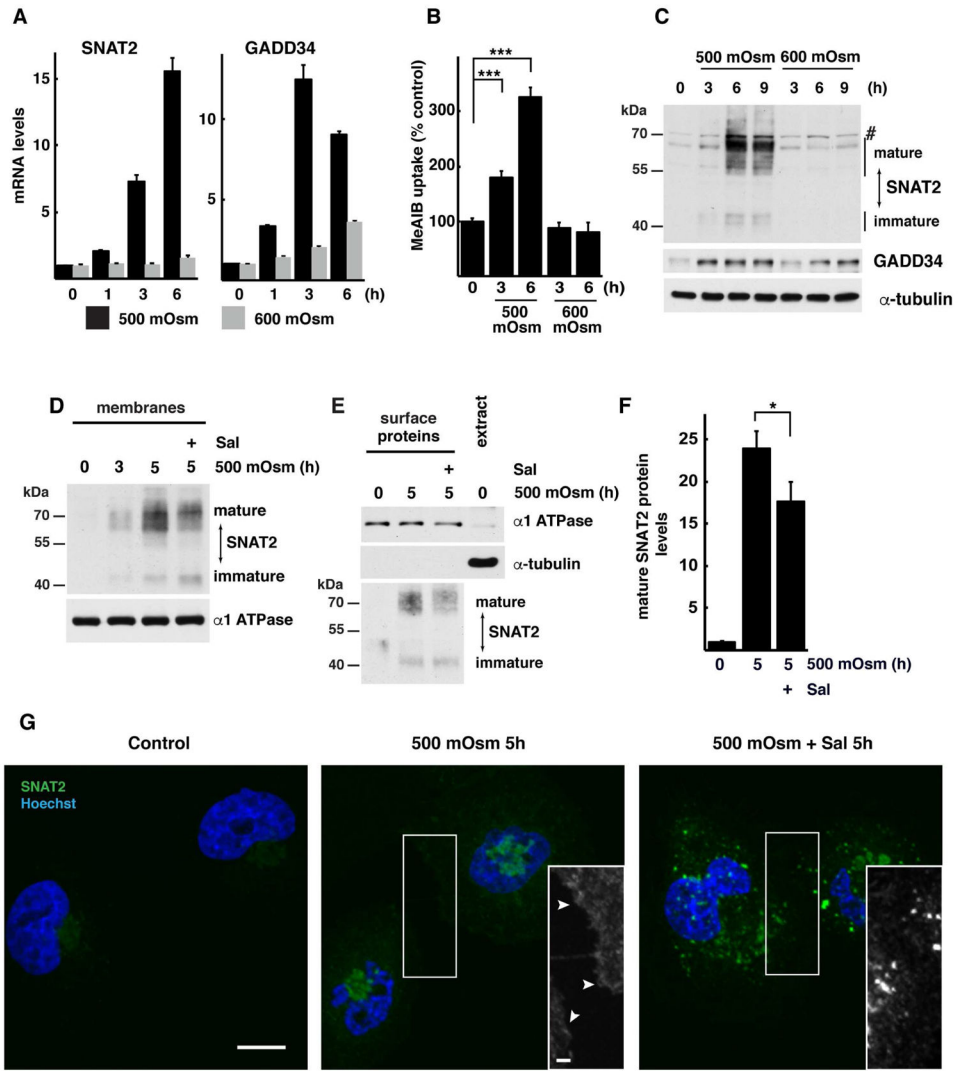

Fig. 1. Adaptation of human corneal epithelial cells to hyperosmotic stress involves SNAT2 and GADD34 induction

A. RT-qPCR analysis of mRNAs from cells treated with 500 or 600 mOsm media for the indicated times. mRNA levels were normalized to the levels of GAPDH mRNA and presented as a fold of induction over control. **B.** SNAT2 activity, measured by ^{14}C-MeAIB uptake in cells exposed to hyperosmotic media for indicated times. **C.** Immunodetection of SNAT2 and GADD34 proteins in extracts from cells treated with 500 or 600 mOsm media for the indicated times. A nonspecific band on the immunoblot is indicated (#). Positions of protein size markers are indicated. **D.** Western blot analysis of the membrane fraction from cells treated with 500 mOsm media for 5h in the presence of Sal003 (30 μM). Positions of protein size markers are indicated. **E**. Immunodetection of SNAT2 in plasma membrane fractions. Biotinylated surface proteins and cell extract (10 μg) were analyzed by Western blotting. Positions of protein size markers are indicated. **F**. Quantification of mature SNAT2 from Panel E by densitometry. Signal intensities of mature SNAT2 was normalized to α-1 ATPase. **G**. Cellular distribution of SNAT2 (green channel) was visualized by confocal fluorescence microscopy. Nuclei are stained with Hoechst. Black and white inserts show

magnification of boxed image areas with green channel signal to demonstrate SNAT2 on plasma membrane (white arrowheads). Scale bars are 10 μm (main image) and 2 μm (insert). Data in panels A,B and F are represented as mean of 3 independent experiments ± SD.

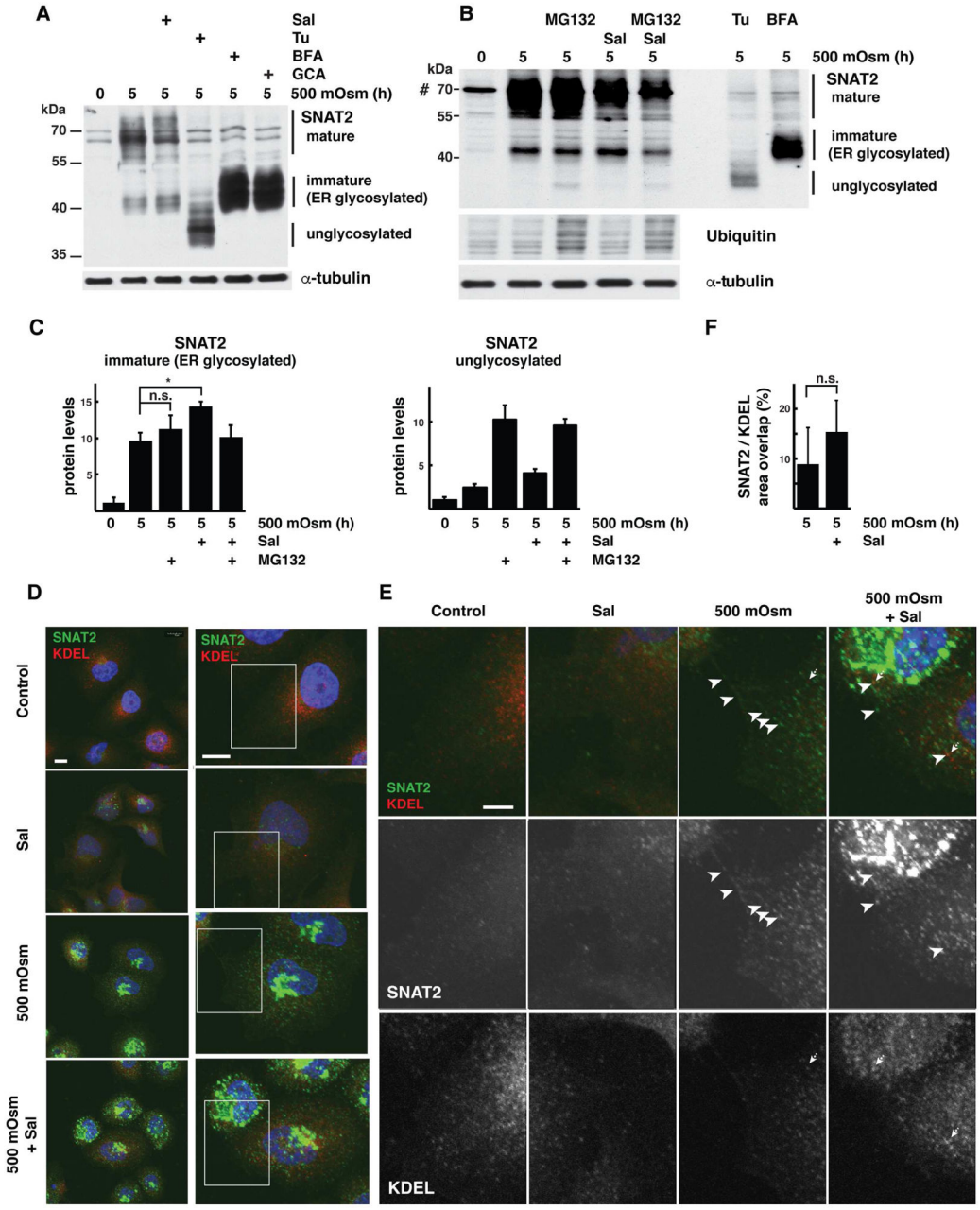

Fig. 2. Hyperosmotic stress-induced GADD34/PP1 activity promotes post-ER SNAT2 protein processing in corneal epithelial cells

A. Western blot analysis of extracts from cells treated with 500 mOsm media alone for 5h or supplemented with Sal003 (30 μM), Tunicamycin (Tu, 500 nM), Brefeldin A (BFA, 20 μM) or Golgicide A (GCA, 20 μM). Positions of protein size markers are indicated. **B.** Western blot analysis of total cell extracts from cells treated with 500 mOsm media for 5h with or without Sup. Sal003 (30 μM). MG132 (100 μM) was added for the last 1h of treatment. Cell extracts from cells treated with 500 mOsm media and Tunicamycin (Tu) or Brefeldin A (BFA) were analyzed by loading one-third the amount of the other samples. **C.** Quantification of immature (left) and unglycosylated (right) SNAT2 levels from cells treated

as in panel B. Signal intensities were normalized to α-tubulin. **D.** Subcellular distribution of SNAT2 (green channel) and ER-resident proteins (red channel, visualized by anti-KDEL antibody staining) in cells grown in control or 500 mOsm media for 5h with or without Sal003 (30 μM) addition. Scale bars are 10 μm. **E.** Boxed image areas from panel D, white arrowheads indicate SNAT2 protein, dotted arrows point to KDEL-positive structures. Scale bar is 1 μm. **F.** Quantification of SNAT2 co-localization with KDEL reporter in cells exposed to 500 mOsm media with or without Sal003. Masks of SNAT2 and KDEL signals were created and overlap between areas was calculated in 4 separate planes. 9 and 11 cells were analyzed respectively. Data re represented as mean ± SD.

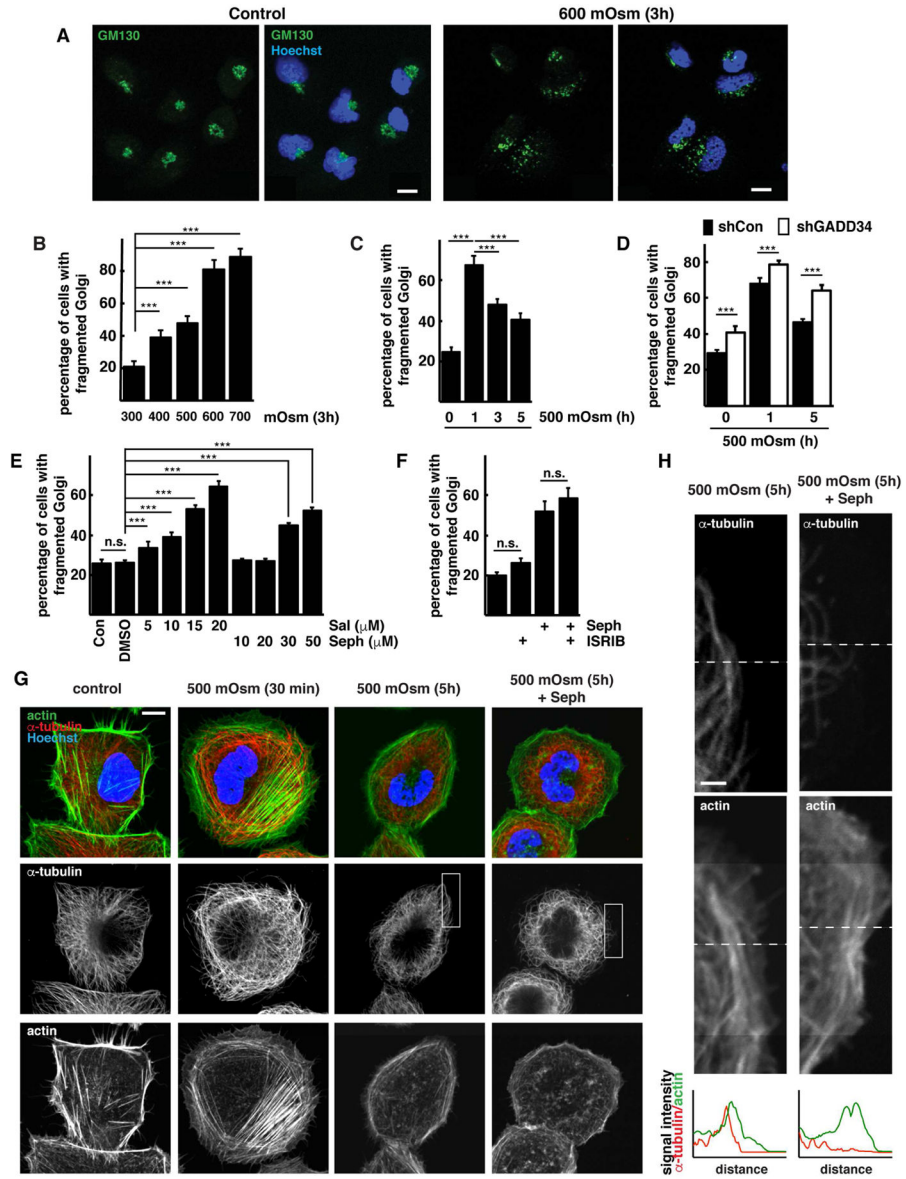

Fig. 3. Osmoprotective functions of GADD34/PP1 in corneal epithelial cells are mediated through reversion of hyperosmotic stress-induced Golgi apparatus fragmentation

A. Immunofluorescent staining of GM130 (green channel) in cells incubated in control or hyperosmotic (600 mOsm) media for 3h. Scale bar is 10 μm. **B.** Quantification of Golgi fragmentation in cells incubated at the indicated conditions for 3h. **C.** Quantification of Golgi fragmentation in cells exposed to 500 mOsm media for the indicated times. **D.** Quantification of Golgi fragmentation in cells expressing shRNA against GADD34 incubated in 500 mOsm media. **E.** Quantification of Golgi fragmentation in cells treated with the indicated concentrations of GADD34/PP1 inhibitors in control media for 2h. **F.** Quantification of Golgi fragmentation in cells treated with the GADD34/PP1 inhibitor Sephin 1 (Seph, 50 μM) with or without ISRIB (25 nM) for 2h. **G.** Immunofluorescent staining of F-actin (green channel) and α-tubulin (red channel) in cells exposed to 500 mOsm media with or without the GADD34/PP1 inhibitor Sephin 1 (Seph, 50 μM). Scale bar

is 10 μm. **H.** Boxed images from panel F. Dotted lines on the images indicate linescans positions. Graphs below are representing α-tubulin (red) and F-actin (green) signals. Scale bar is 2 μm. Data in panels B–F are represented as mean of 3 experiments ± SD.

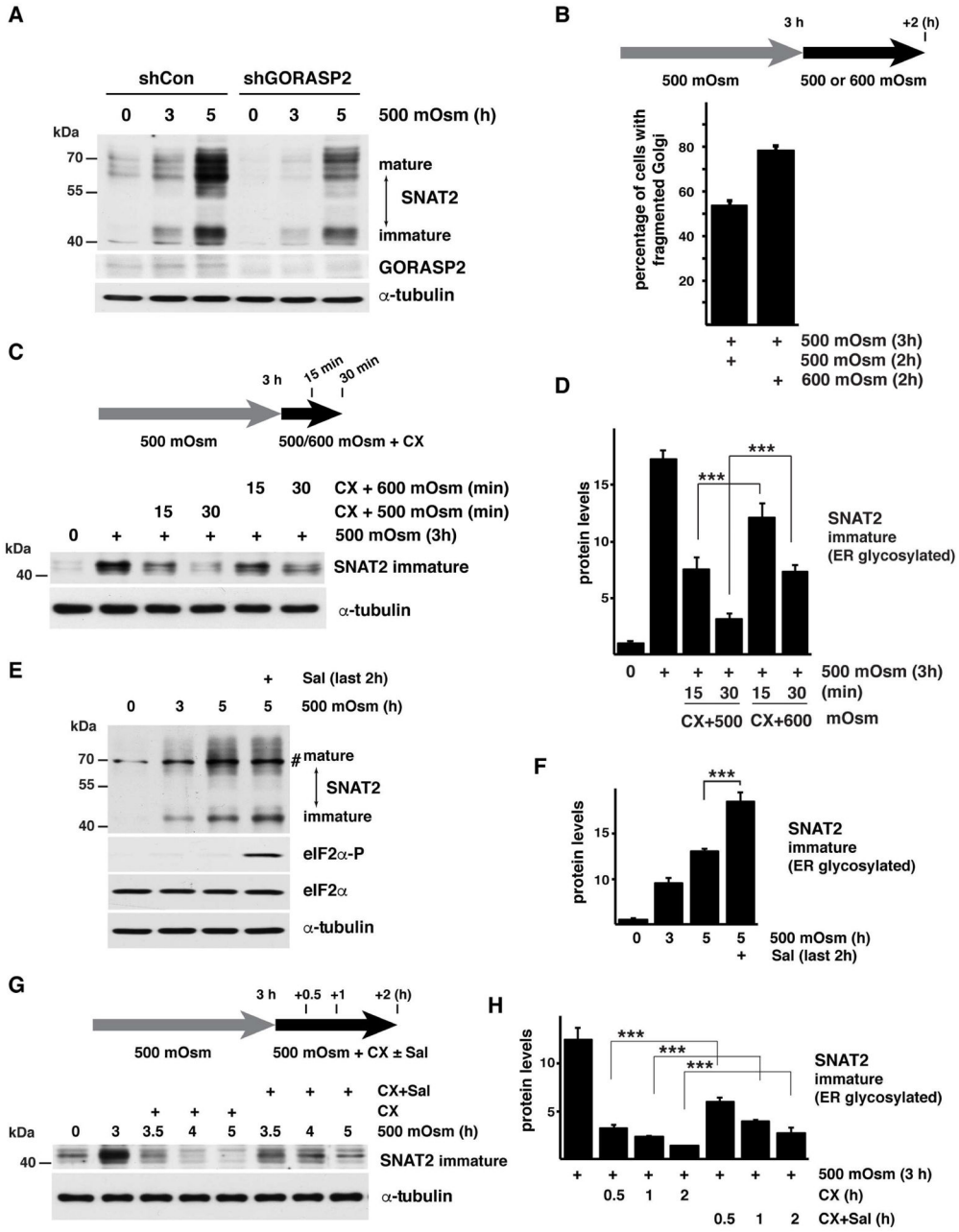

Fig. 4. Golgi apparatus fragmentation delays SNAT2 maturation in corneal epithelial cells

A. Western blot analysis of extracts from cells expressing shRNA against GORASP2 exposed to hyperosmolar stress. Positions of protein size markers are indicated. **B.** Quantification of Golgi fragmentation in cells treated with 500 mOsm media for 3h and then switched to 500 or 600 mOsm media for additional 2h. **C.** Western blot analysis indicating the immature form of SNAT2 from cells treated with 500 mOsm media for 3h and then switched to 500 or 600 mOsm media in the presence of CX for the indicated times. **D.** Quantification of the data from panel C. SNAT2 signal intensities were normalized to α-tubulin **E.** Western blot analysis of extracts from cells cultured in 500 mOsm media for 5h

with Sal003 (30 μM) added for the last2 h. A nonspecific band is indicated (#). **F.** Quantification of the immature SNAT2 levels from cells treated as in E as described above. SNAT2 signal intensities were normalized to α-tubulin. **G.** Western blot analysis showing the immature form of SNAT2 from cells treated with 500 mOsm media for 3h. The cells were then incubated with CX and Sal003 for the indicated times. **H.** Quantification of immature SNAT2 levels from cells treated as in G as described above. SNAT2 signal intensities were normalized to α-tubulin. Data in panels B, D, F, and H are represented as mean of 3 experiments ± SD.

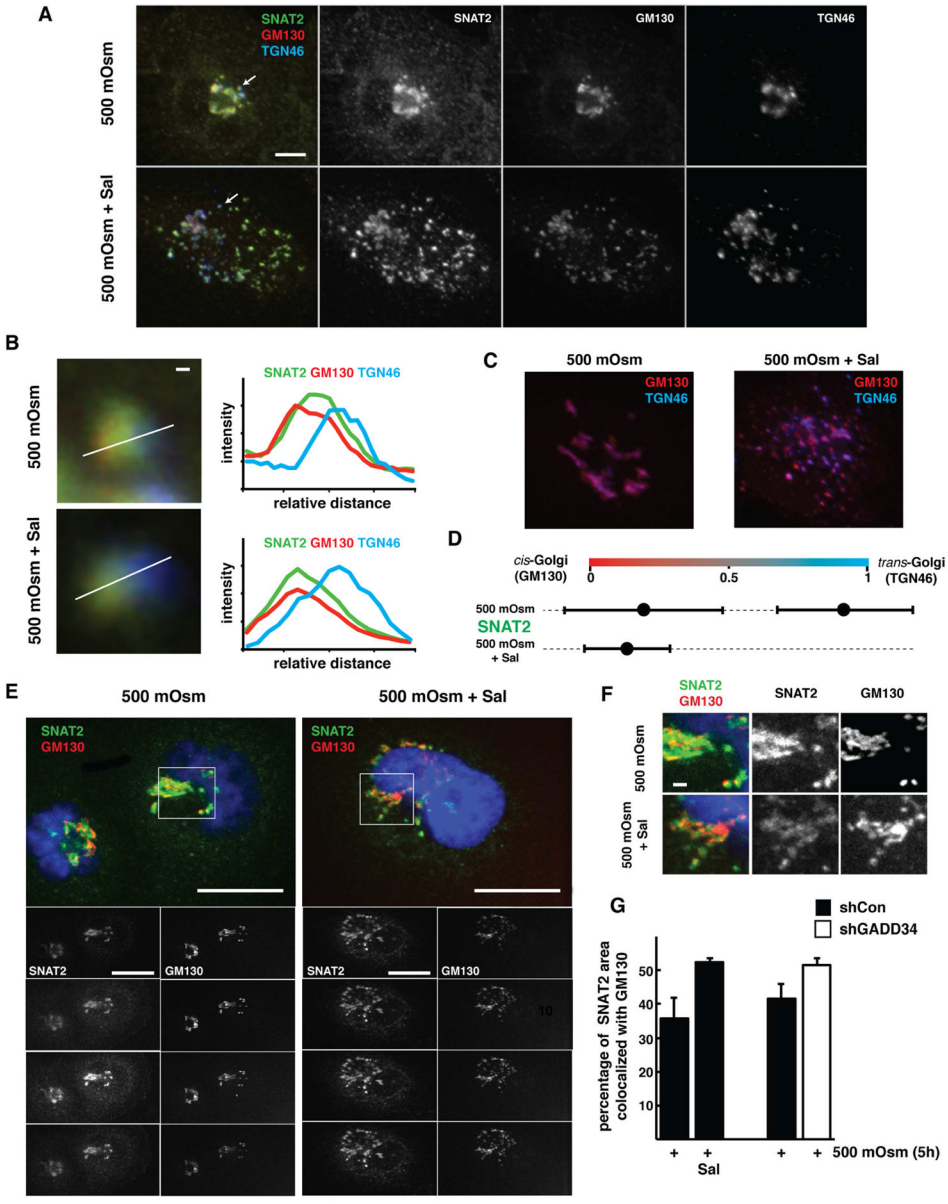

Fig. 5. Inhibition of GADD34/PP1 results in the SNAT2 retention in *cis*-Golgi in corneal epithelial cells exposed to hyperosmotic stress

A. Intra-Golgi localization of SNAT2, where *cis*-Golgi marker is GM130 and *trans*-Golgi marker is TGN46; in cells treated with 500 mOsm media with or without Sal003 (30 μM) for 5h. Arrows point to the areas enlarged in B. Note Golgi fragmentation and separation of *trans*-Golgi blue color from SNAT2 and GM130 in Sal003 treated cells. Scale bar is 10 μm. **B.** Linescan analysis of SNAT2 intra-Golgi localization, with representative examples of linescanes and plots of three channel intensities through regions with separated *cis*- and *trans*-Golgi. Scale bar is 1 μm. **C.** Representative Golgi morphology and overlap between *cis*- and *trans*-Golgi staining in 500 mOsm cell treated with or in absence of Sal003. **D.** Graph represents quantitation of analysis of 14 line scans from 6 cells treated with 500 mOsm media and 45 linescans taken from 14 cells treated with 500 mOsm media in the

presence of Sal003 (30 μM) respectively. Data are represented as mean ± SD. **E.** Subcellular localization of SNAT2 and *cis*-Golgi marker GM130 in cells treated with 500 mOsm media for 5h with or without Sal003 (30 μM). Scale bar is 10 μm. **F.** Magnifications of cell area as indicated in panel E. Note SNAT2 areas that do not overlap with GM130 staining in 500 mOsm treated cells, and their disappearance upon Sal003 addition. Scale bar is 1 μm. **G.** Quantification of SNAT2 area overlapping with GM130. Data are represented as mean of 3 experiments ± SD.

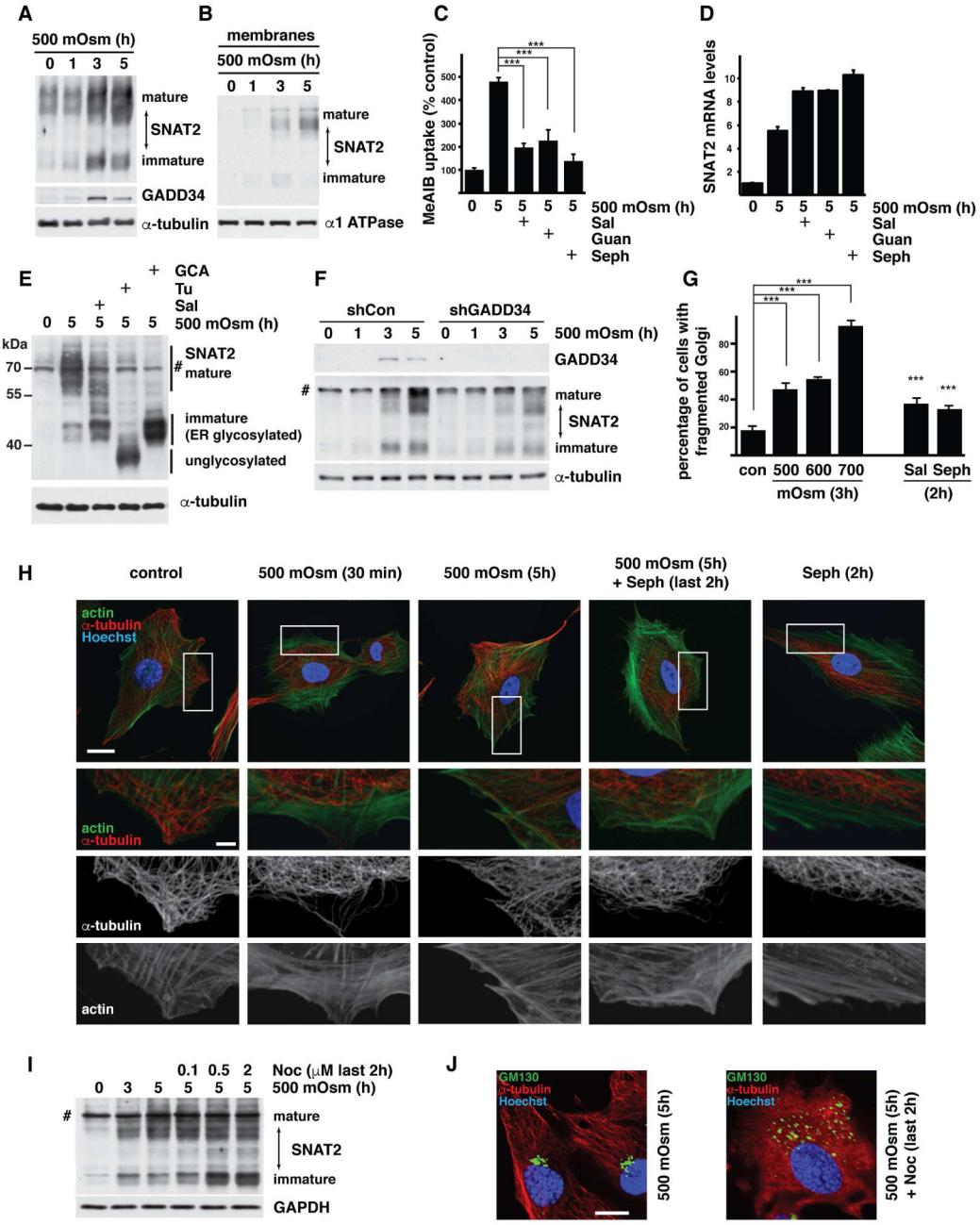

Fig. 6. GADD34 promotes SNAT2 maturation independently from the eIF2α phosphorylation status in mouse embryonic fibroblasts

Experiments were conducted in mouse embryonic fibroblasts expressing mutated eIF2α protein (S51A MEFs). A. Immunodetection of SNAT2 protein in extracts from cells exposed to 500 mOsm media for the indicated times. B. Immunodetection of SNAT2 in membrane fractions from cells treated as in panel A. C. ^{14}C-MeAIB uptake in cells exposed to 500 mOsm media for 5h with or without Sal003 (30 μM) Sephin 1 (Seph, 100 μM) or Guanabenz (Guan, 100 μM). D. RT-qPCR analysis of SNAT2 mRNA levels from cells treated with 500 mOsm media for 5h in the presence of GADD34/PP1 inhibitors. Values were normalized to

GAPDH mRNA and are plotted as a fold of induction over control. E. Western blot analysis of extracts from cells treated with 500 mOsm media for 5h in the presence of Sal003 (30 μM), Tunicamycin (Tu, 500 nM) or Golgicide A (GCA, 20 μM). A nonspecific band is indicated (#). Positions of protein size markers are marked. F. Western blot analysis of extracts from cells expressing shRNA against GADD34 and treated with 500 mOsm media. G. Quantification of Golgi fragmentation in cells incubated in the indicated stress conditions for 3h or treated with GADD34/PP1 inhibitors Sal003 (30 μM) or Sephin 1 (Seph, 50 μM) in control media for 2h. H. Immunofluorescent staining of F-actin (green channel) and α-tubulin (red channel) in control cell and after exposure to 500 mOsm media with or without Sephin 1 (Seph, 50 μM). Upper panel Scale bar is 20 μm. 3 lower panels represent magnification of boxed areas from the upper panel, with scale bar 5 μm. I. Immunodetection of SNAT2 protein in extracts from cells incubated in 500 mOsm for 5h with the indicated concentrations of nocodazole during the last 2h of treatment. J. Immunofluorescent staining of α-tubulin (red channel) and the Golgi marker-GM130 (green channel) in cells treated with 500 mOsm stress with or without nocodazole (Noc, 2 μM). Scale bar is 20 μm. Data in panels C and G are represented as mean of 3 experiments ± SD

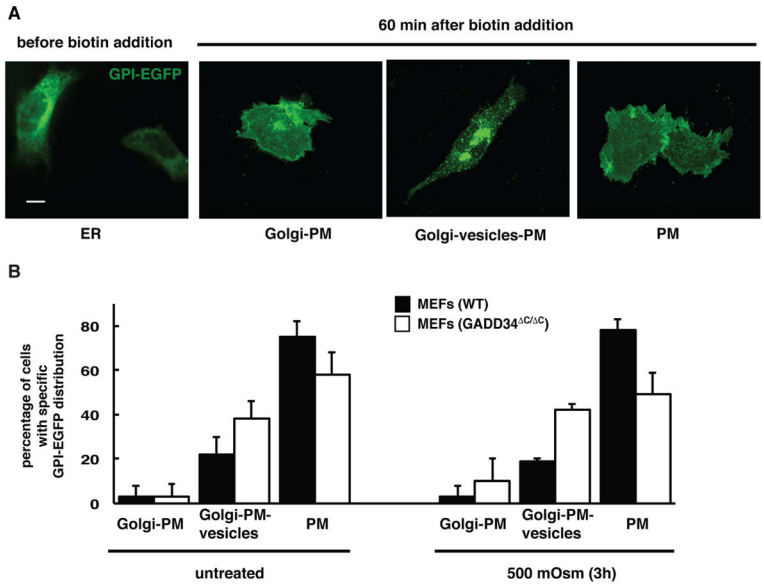

Fig. 7. GADD34 promotes GPI-EGFP protein trafficking in MEFs

A. Examples of images showing GPI-EGFP distribution in WT MEFs before and after cargo release from the ER with biotin addition (40 μM). Scale bar is 10 μm. **B.** Quantification of GPI-EGFP distribution in WT and GADD34 $^{\Delta C/\Delta C}$ MEFs 60 min after biotin addition (40 μM). Data are represented as mean ± SEM.